Biochemical Engineering Journal 227 (2026) 110037

Contents lists available at ScienceDirect

Biochemical Engineering Journal

journal homepage: www.elsevier.com/locate/bej

Regular article

Addressing temperature gradient challenge in scaling up solid-state fermentation: A strategy using thermophilic strains for biosurfactant production

Jose Bueno-Mancebo, Adriana Artola, Syeda Amna Farooq, Raquel Barrena *, Teresa Gea

Composting Research Group, Department of Chemical, Biological and Environmental Engineering, Escola d'Enginyeria, Universitat Autònoma de Barcelona, Cerdanyola del Vallès, Barcelona 08193, Spain

ARTICLE INFO

Keywords:
Lipopeptide
Bacillus subtilis
Thermophiles
Biosurfactants
Biowaste

ABSTRACT

Solid-state fermentation (SSF) is a promising approach for sustainable bioproduction production, particularly when using organic waste as a substrate. However, temperature gradients inherent to large-scale SSF often reduce process efficiency. This study developed a strategy for designing of a lipopeptide biosurfactant production process, scaling SSF in packed-bed bioreactors by thermophilic strains using winterisation oil cake (WOC) and sugarcane molasses (MOL) as nutrient sources. Fermentations at lab-scale (0.5 L) and pilot-scale (50 L) demonstrated a robust and reproducible process despite temperature changes from microbial activity. Among the strains tested, *Bacillus subtilis* CBI-7S1 was the highest producer, with optimal substrates amounts of 24 g of WOC and 12 g of MOL, producing 24.9 mg of crude lipopeptides per gram of dry matter (DM) at 0.5 L scale. These conditions were reproduced at pilot scale, with concentrations from 12 to 24 mg g^{-1} DM. Moisture content strongly influenced biosurfactant production, while oxygen consumption was a reliable monitoring parameter. Surface tension was evaluated under different pH, temperature, and salinity, and mass spectrometry identified surfactin, iturin, and fengycin congeners. These findings provide insights into overcoming temperature gradients during scale-up and show that thermophilic strains enable biosurfactant production under SSF at pilot scale. This approach enhances SSF technological maturity, supporting its broader use in sustainable production of targeted metabolites across diverse bioprocesses.

1. Introduction

The production of biosurfactants involves the conversion of various organic substrates into surface-active compounds through microbial metabolism [1]. However, the high production costs, primarily due to the use of refined substrates, have limited the widespread adoption of biosurfactants in industrial applications.

Solid-state fermentation (SSF) is a process in which microorganisms grow on moist solid substrates without free-flowing water, using the substrate both as a physical support and a source of nutrients, and has been explored as an alternative for biosurfactant production [2]. This technology offers potential for large-scale implementation by utilising organic by-products as substrates [3]. Despite the economic and environmental advantages of reduced feedstock costs in an SSF process, challenges such as heat and mass transfer limitations, and heterogeneity inside the reactor remain significant obstacles for efficient large-scale production of any type of bioproduct, including biosurfactants [4,5].

One of the critical challenges in operating large-scale packed bed bioreactors for SSF is managing temperature gradients resulting from metabolic heat release, which is a common issue particularly at pilot and industrial scales [6]. High temperatures within the solid matrix can negatively impact microbial growth and targeted metabolite production. To address overheating, increasing the airflow rate could be a strategy for SSF. However, increasing airflow increases energy costs and may reduce the moisture content of the substrate to suboptimal levels, which can limit microbial activity and growth. Although complete drying is unlikely, even moderate moisture loss can affect the fermentation process by shifting the system away from the optimal range for microbial metabolism [7]. This, in turn, affects microbial activity and reduces metabolite yields, with moisture loss becoming a bottleneck for bioproduct production in SSF processes.

Overcoming these challenges requires strategic substrate selection

* Corresponding author.
E-mail address: raquel.barrena@uab.cat (R. Barrena).

https://doi.org/10.1016/j.bej.2025.110037
Received 3 September 2025; Received in revised form 21 November 2025; Accepted 1 December 2025
Available online 2 December 2025

and the use of robust microbial strains. The use of thermotolerant or thermophilic microorganisms can enhance the feasibility of SSF by supporting growth at higher temperatures while tolerating local temperature variations within the substrate. These microorganisms maintain metabolic activity despite these differences, making them suitable for SSF under elevated temperatures. While not a scale-up strategy per se, employing such strains is a microbiological design choice that facilitates operation at larger scales, thereby supporting the commercialisation of SSF technology [8–11].

Agro-industrial residues provide nutrient-rich materials that support microbial activity while reducing process costs and industrial waste to be treated, making them ideal candidates as SSF substrates. This approach aligns with waste management initiatives and the circular bioeconomy model policies outlined by the European Commission [12]. A wide range of agricultural residues and agro-industrial waste serve as suitable substrates for SSF. Oil cakes, known for their rich hydrophobic carbon content, are frequently reported as SSF substrates in biosurfactant production [13–15]. Recently, we isolated several thermophilic, biosurfactant-producing strains capable of utilising organic waste as a growth substrate. Among them, the most promising were identified as *Bacillus* species producing lipopeptides [16].

This study represents a further step toward enabling the scale up of SSF and, for the first time, applies the use of thermophilic microorganisms for biosurfactant production under these conditions. To this end, we will explore the use of different thermophilic biosurfactant producer strains in SSF using a mixture of agro-industrial residues as the nutrient source. The process was first studied and optimised at laboratory scale under controlled temperature conditions. Subsequently, the strategy was tested at pilot scale using a 50 L thermally insulated bioreactor. In this setup, temperature evolved naturally leading to the development of temperature gradients within the reactor.

2. Materials and methods

2.1. Fermentation strain and preparation of seed culture

Three thermophilic strains were used in this study: *Bacillus subtilis* (CBI-7S1 and TBCE-7S3) and *Bacillus licheniformis* (GFS-S3). These strains were previously isolated by our research group during a preliminary study aimed at identifying thermophilic microorganisms capable of producing biosurfactants [16]. They were isolated from a community composting system treating biowaste at a primary school in Barcelona, during the thermophilic phase of the composting process (50ºC). For the current experiments, the strains were cultivated using nutrient broth and malt extract agar media sterilised at 121°C for 20 min [16]. Seed cultures were prepared in 500 mL Erlenmeyer flasks containing 100 mL of nutrient growth media and incubated at 50°C and 180 rpm for 20 h. The prepared seed solution was used as inoculum for SSF in subsequent experiments.

2.2. SSF substrates

The initial solid mix for each SSF experiment consisted of wheat straw, winterisation oil cake (WOC), sugarcane molasses (MOL), all sourced from local providers, or commercial glucose as a control in the strain screening (Fig. S1). Wheat straw, obtained from the Veterinary Faculty of the Autonomous University of Barcelona (UAB), was used as the solid support and had a moisture content of 5.6 % (wet matter basis). MOL, a byproduct of the sugar refining industry, was provided by AB Azucarera Iberia S.L.U. (Madrid, Spain) and had a moisture content of 17.1 % (WM basis) and a sugar content of 44 % (g sugar per g sample). WOC, produced by crystallising waxes from sunflower oil at temperatures below −5°C and filtering with perlite, was supplied by Lípidos Santiga, S.A. (Barcelona, Spain). WOC had a moisture content of 4.4 % (WM basis) and a fat content of 44 % (dry matter basis). Wheat straw, WOC and MOL were sterilised at 121°C for 20 min before reactor loading.

2.3. Screening of carbon source for thermophilic strains

A screening was conducted to evaluate whether the three strains could grow and produce crude lipopeptide biosurfactant (LPc) using molasses as an alternative carbon source to glucose. To maintain aerobic conditions without forced aeration, cultures were grown in 0.5 L Erlenmeyer flasks filled to one-third of the total volume, preventing bed compaction and providing ample headspace for passive oxygen diffusion. Flasks were closed with breathable plugs and incubated at 50°C for 4 days [16]. The total weight of the solid substrate was approximately 55.1 ± 0.2 g, with a dry matter content of 19.2 % of the total weight. The solid matrix comprised 7.28 g of wheat straw as a support material, 5.4 g of WOC, as a hydrophobic carbon source, and 20 mL of molasses or glucose solution as a hydrophilic carbon source (equivalent to 0.4 g of total sugars in the initial mixture) [17]. Minimal salt medium (MSM) was used according to [16], consisting of yeast extract (1 g L^{-1}), NH_4NO_3 (1 g L^{-1}), $MgSO_4$ (0.2 g L^{-1}), KH_2PO_4 (1 g L^{-1}), K_2HPO_4 (1 g L^{-1}), $FeCl_3$ (0.05 g L^{-1}), NaCl (0.05 g L^{-1}) and glucose (2 g L^{-1}). A total of 16 mL of this medium was added, resulting in an initial moisture content of approximately 65 %. The medium was supplemented with 6.6 mL of inoculum, prepared to an optical density of 1.5 at 600 nm, corresponding approximately to total 10^6 initial colony formation units (CFU), to initiate the fermentation process.

2.4. Solid-state fermentation system at laboratory scale

SSF experiments were done in 0.5 L packed-bed reactors under sterile conditions. All reactors were filled with 14 g of wheat straw, 30.7 mL of MSM, 12.7 mL inoculum, WOC and MOL in different proportions according to the experiment (Table 1). Purified water was added to adjust the moisture content to 65.7 % (corresponding to 75 % of the water holding capacity of the mixture, water basis). The average initial weight across all conditions was 102.8 ± 0.5 g. The experimental setup is depicted in Fig. 1. The fermentation reactors were incubated in a thermostat water bath at 30, 40, 50, or 60°C for 4 days.

A continuous humidified airflow was supplied from the base of each reactor using a mass flow controller (Bronkhorst, Netherlands), ensuring that the solid matrix remained moist throughout the fermentation. The air passed upwards through the solid bed and exited at the top. The airflow rate was set at 30 mL min^{-1}, equivalent to 35.3 L h^{-1} kg^{-1} DM. Oxygen levels in the exhaust gases were monitored using an electrochemical oxygen sensor (Alphasense, UK). An Arduino®-based system connected to the sensors recorded oxygen concentrations in real time and calculated the specific oxygen uptake rate (sOUR) using the following equation (Eq.1):

Table 1
Factorial design matrix and response (lipopeptide crude, LPc) values for varying ratios and quantities of sugarcane molasses (MOL) and winterisation oil cake (WOC) as substrates.

Run	Variables		*Bacillus* growth (ΔlogCFU)	LPc production		
	MOL (g)	WOC (g)		(total g)	(mg g^{-1} substrate)	(mg g^{-1} DM)
1	24	6	2.96	0.62	20.7	17.6
2	12	12	3.53	0.52	21.7	17.1
3	12	6	3.14	0.45	25.0	11.3
4	12	12	3.52	0.52	21.7	14.1
5	12	12	3.49	0.54	22.5	16.5
6	24	6	3.11	0.60	20.0	16.5
7	12	6	3.18	0.67	37.2	18.1
8	24	12	2.81	0.88	24.4	23.9
9	12	6	3.20	0.80	44.4	21.0
10	24	12	2.91	1.08	30.0	30.6
11	24	12	2.78	1.10	30.6	28.6

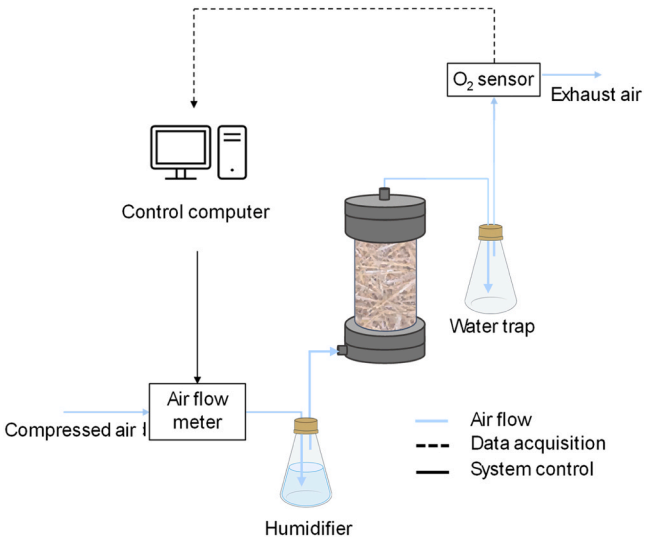

Fig. 1. Schematic 0.5 L packed-bed reactor system.

$$sOUR = \frac{\Delta O_2 \cdot F \cdot 31.98 \cdot 60 \cdot 1000^{a}}{1000^{b} \cdot 22.4 \cdot DM} \quad (1)$$

where sOUR represents the oxygen uptake rate (mg O_2 g^{-1} DM h^{-1}); ΔO_2 is the difference in oxygen concentration between the inlet and outlet air, expressed as a volumetric fraction; F is the airflow rate (mL min^{-1}); 31.98 is the molecular weight of O_2 (g mol^{-1}), and 60 converts minutes to hours. The terms (1000^a) and (1000^b) adjust units from mg to g and mL to L, respectively. The constant 22.4 refers to the molar volume of an ideal gas under standard conditions (L), and DM is the dry matter weight of the substrate in the reactor (g).

The cumulative oxygen consumption (COC), expressed in g O_2 per g DM, was calculated by integrating the oxygen consumption curve. This metric provided insights into the overall biological activity within the reactors [18].

To optimise the ratio and quantity of hydrophobic (WOC) and hydrophilic (MOL) carbon sources, a factorial experimental design comprising eleven runs was conducted at 50°C. The substrate proportions (w w^{-1}) tested were 4:1, 2:2, 2:1, and 4:2 (WOC:MOL), where one unit corresponded to 6 g of substrate. Data were analysed using the statistical software Design-Expert 12® program (Stat-Ease, Inc., United States). The program was used to predict the optimal conditions for maximising crude biosurfactant production. Validation experiments were subsequently carried out in triplicate under the predicted optimum conditions.

The influence of temperature on microbial growth and lipopeptide production was also investigated under the optimised substrate mixture. A total of twelve reactors were prepared and operated under optimised conditions and distributed into four triplicate sets, each incubated at 30, 40, 50, or 60°C in separate controlled water baths.

2.5. Solid-state fermentation at pilot scale

A thermally insulated reactor with a 50 L working volume was used in this study, as illustrated in Fig. 2 A. The fermenter is a cylindrical, stainless-steel vessel. A perforated metal plate at the bottom of the reactor both supports the solid matrix and separates it from the air distribution chamber (Fig. 2B). This design prevents obstruction at the air inlet and helps for a uniform air distribution throughout the solid matrix [19]. This reactor features a diameter-to-height ratio of 0.612, and its lateral wall is thermally insulated, minimising heat dissipation and helping to maintain temperature conditions similar to those that could occur at the centre of the mixture in a large-scale bioreactor.

The composition of the solid matrix followed the same proportions as the laboratory-scale experiments and was based on the results of the optimised conditions, with a slight modification. Wheat straw (1 kg) was used as the support material, together with wood chips (2.3 kg) as a bulking agent to prevent excessive compaction of the mixture, along with 1.7 kg of WOC, 3 L of MSM, 0.9 L of molasses, and 3.8 L of water (all sterilised) and 0.9 L of inoculum. This mixture reached a height of 42.5 cm inside the reactor, with a diameter of 35 cm. At the end of fermentation (4 days), the mixture was manually collected from the reactor at specific locations for subsequent analyses.

Forced aeration was used, with the airflow adjusted to maintain a flow of 20.4 L kg DM^{-1} h^{-1}, ensuring aerobic conditions. The airflow was humidified by passing it through a humidifier set at 60°C. This prevented a temperature drop inside the reactor caused by cooler ambient air. Air was supplied through a flowmeter (Bronkhorst, Netherlands), exiting through the top, and then directed to an oxygen sensor. Temperature was monitored using button sensors (standard Thermochron iButton device, Maxim Integrated, U.S.) positioned throughout the reactor. These sensors were placed within the solid mix

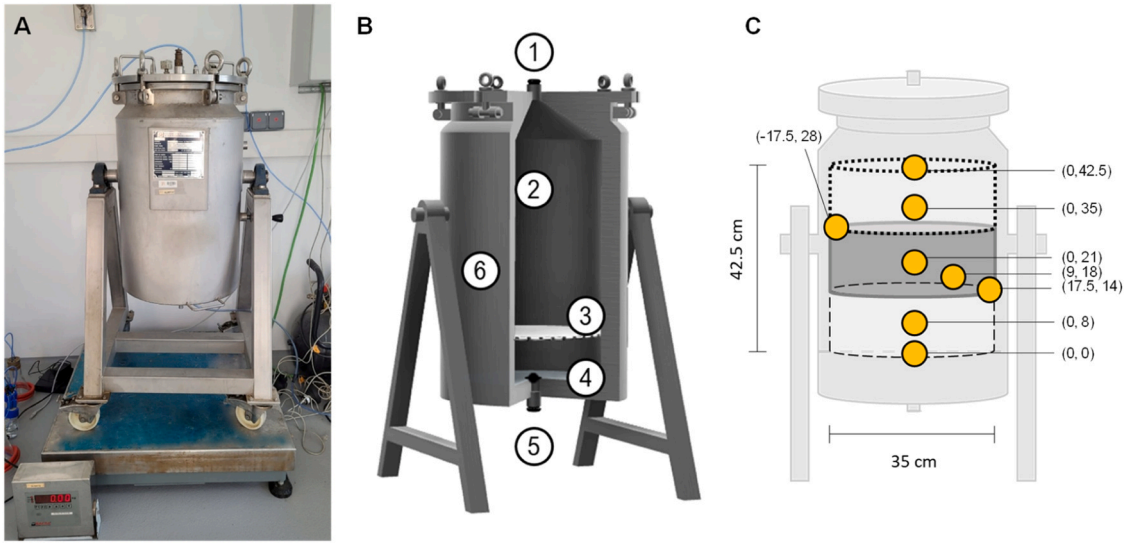

Fig. 2. (A) Photograph of the 50 L reactor. (B) 3D representation of the 50 L packed-bed reactor. 1. Airflow outlet; 2. Fermentation chamber; 3. Metallic mesh; 4. Air chamber; 5. Airflow inlet; 6. Thermally insulated wall. (C) Distribution of temperature sensors in the reactor.

to measure the temperature inside the packed bed. They were set at heights of 0, 8, 21, 35, and 42.5 cm at the centre, at 14 and 18 cm near the wall (Fig. 2 C).

Oxygen consumption was monitored using the same system used at laboratory scale. A portable multisensor (POLI Multi-gas detector, mPower Electronics) was used for gaseous compounds measurement, equipped with an electrochemical sensor for NH_3 measurement (detection range from 0 to 500 ± 1 ppmv), an electrochemical sensor for H_2S measurement (detection range from 0 to 100 ± 0.1 ppmv) and a photoionization detector for total total volatile organic compounds (VOC) measurement (detection range from 0 to 2000 ± 0.1 ppmv). All concentrations are reported as ppmv (parts per million by volume, μmol of gas per mol of air).

2.6. Analytical methods

The number of viable cells was estimated through colony-forming unit (CFU) counts, following the method described by [20]. Briefly, 10 g of fermented solid was mixed with 90 mL of Ringer® sterile saline solution in an orbital incubator at 200 rpm, 25ºC for 20 min. Serial dilutions were carried out (1:10, w v^{-1}) and 100 μL of each dilution was inoculated and spread on agar plates and incubated at 50ºC for 48 h. After incubation, the CFU were counted using the Schuett counter (Göttingen, Germany). The parameters such as moisture content and pH were characterised according to standard procedures [21].

LPc extraction was performed using water as the extraction solvent to avoid organic compounds, following the acid precipitation method described by [22,23], with slight modifications. 10 g of fermented solid was mixed with distilled water (1:10, w v^{-1}) and adjusted to pH 8 with NaOH solution. The mixture was incubated at 25°C for 1 h at 180 rpm, then centrifuged at 10,000 rpm and 4 °C for 20 min. The pH of the liquid extract was adjusted to 2 by adding 3 M hydrochloric acid, and the acidified mixture was stored overnight at 4°C. The precipitated biosurfactant was separated from the liquid phase by centrifugation under the same conditions, resuspended in distilled water, and lyophilised for further analysis. After extraction, the residual solid phase remained suitable for further valorisation, such as anaerobic digestion or composting, thus integrating the process within a circular bioeconomy framework.

For UHPLC–ESI–MS analysis (Agilent 1200 UHPLC coupled to a Bruker timsTOF Pro 2, positive ion mode), lyophilised LPc was diluted 1:10 (w v^{-1}) in methanol, mixed, and centrifuged (10,000 rpm, 15 min, 4°C) [24]. Then, 10 μL were injected onto a C18 column (4.6 × 100 mm, 120 Å). Isocratic elution was performed at 30°C and 1 mL min^{-1} with 70 % acetonitrile in 1 % formic acid and 30 % water in 1 % formic acid for 30 min.

The surface tension (ST) of LPc extracts from the central upper area of the 50 L reactor was determined using the Wilhelmy Plate method with a Krüss tensiometer (Hamburg, Germany) at room temperature. To evaluate the surface activity of the liquid extract, 30 mL of the sample was collected and diluted in various proportions with distilled water. The critical micelle concentration (CMC) was determined by plotting the ST values against the concentration of LPc resuspended in water, identifying the point where further dilution no longer reduced the ST. The LPc stability was evaluated through ST measurement at different pH (2−12), temperatures (4, 37, 58, 83, 105ºC) and NaCl concentrations (5–20 w v^{-1}). All measurements were performed at 23°C and near-neutral pH, except during the respective temperature and pH experiments. The ST measurements for the characterisation of LPc correspond to the mean of 10 experimental readings per sample.

2.7. Statistical analysis

Means were compared using Tukey's test with 95 % confidence by SigmaPlot 12.5 (Systat Software Inc., San Jose, California, United States). Results from the strain screening were obtained in duplicate fermentations, while those from the temperature evaluation experiment were obtained in triplicate. A factorial randomised design was implemented to optimise the amount of WOC and MOL for biosurfactant production. Analysis of variance (ANOVA) was used to evaluate the significance of fit for the model equations. The experimental results were fitted to a factorial model, and ANOVA was performed to determine the statistical significance of the model terms. Moisture content, pH, CFU and LPc are presented in the manuscript as mean and standard deviation of the means for triplicate.

3. Results and discussion

3.1. Thermophilic strain selection for lipopeptide production by SSF

Initially, we evaluated the ability of the three isolated thermophilic Bacillus strains to produce biosurfactants in SSF. Two hydrophilic carbon sources, glucose and MOL, were compared in duplicates. Fig. 3 shows higher growth and lipopeptide production when using MOL over glucose. This is probably due to the presence of additional trace elements and vitamins in this residue, as well as the sugar profile. The presence of other sugars, such as fructose, may enhance *Bacillus*' efficiency in nutrient uptake [25,26].

Although GFS-S3 showed higher cell growth, the CBI-7S1 strain was selected for subsequent experiments due to its higher production under the same conditions as the other strains.

3.2. Solid-state fermentation process in 0.5 L packed-bed reactors

3.2.1. Effect of carbon source ratio and load

Biosurfactant production was evaluated in eleven 0.5 L solid-state packed-bed reactors at 50ºC. Hydrophilic (MOL) and hydrophobic (WOC) carbon sources were tested in various ratios, which were previously shown to significantly affect biosurfactant production in SSF [20]. Table 1 presents the experimental data obtained from the fermentation processes.

After 4 days of fermentation, CFUs increased between 2- and 3.5-fold. The final pH values of the cultures ranged from 6.6 to 7.7. Biosurfactant production ranged from 11.3 to 30.6 mg LPc g^{-1} DM, with most values exceeding the maximum concentration obtained during the initial screening (15 mg LPc g^{-1} DM), probably due to more favourable aeration conditions in packed bed bioreactors used herein compared to Erlenmeyer flasks used by [16]. The highest LPc production was observed in runs 8, 10 and 11, achieving an average of 1.0 ± 0.1 g, corresponding to a mixture of 24 g of MOL and 12 g of WOC. In contrast, the lowest production was recorded in the triplicate corresponding to

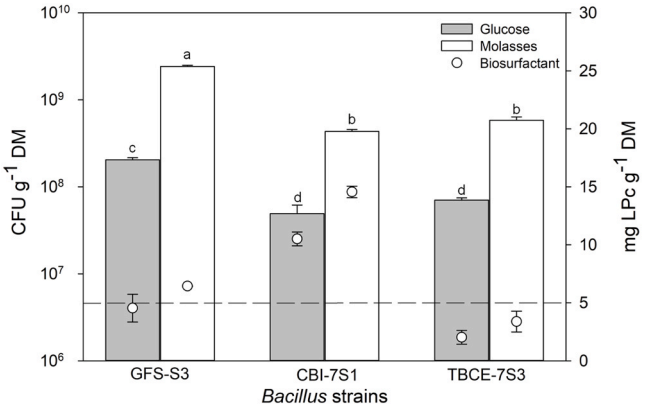

Fig. 3. Preliminary screening results for strain growth and LPc production after 4 days of fermentation at 50ºC. The dashed line indicates the initial CFU per gram of DM. [a, b, c, d] Means that do not share a letter differ significantly ($p > 0.05$).

12 g of MOL and 12 g of WOC. The difference in LPc production between these conditions may be attributed to the higher total substrate availability (36 g vs 18 g), providing more assimilable carbon and nutrients to support cell growth and secondary metabolite production. Given that LPc represents a significant product in this fermentation system, its production likely depends, at least in part, on the availability of substrates that can be converted into precursors for LPc biosynthesis, although regulatory factors in the biosynthetic pathway may also contribute.

The variables were analysed using multiple regression analysis to derive a regression equation capable of predicting the response within the specified range [27]. Analysis of variance (ANOVA) was used to evaluate the significance of fit for the model equations. As the focus of this study is the production of biosurfactant, the following discussion centres on this aspect; statistical analysis applied to viable cells is available in the supplementary information.

The experimental results were fitted to a factorial model. The ANOVA presented in Table 2 indicated that the regression model was significant ($p < 0.05$) and a non-significant lack of fit ($p > 0.05$). Consequently, the model demonstrated a good fit with the experimental data. The parameter WOC and the interaction term AB (the effect of WOC:MOL combination) exhibited significant effects. Based on the R^2 value, which measures the degree of fit, the model explained 82.3 % of the variability in the response.

Eq. (2) shows the regression model for LPc under the studied conditions, where A, B and AB represent the amount of WOC (g), MOL (g) and interaction between them, respectively.

$$\text{LPc (total g)} = 1.440 - 0.052\,A - 0.121B + 0.008AB \quad (2)$$

Using this model, the Design-Expert® software predicted the optimum LPc production at 24 g of WOC and 12 g of MOL. The optimal conditions predicted by the model are consistent with the experimental trends, confirming that higher substrate concentrations, combined with a balanced ratio of WOC and molasses, increase LPc production. However, further increases in substrate loading are limited by the physical properties of the system. Wheat straw can absorb up to 4.5 g of water per gram of dry straw under the conditions used, restricting additional moisture uptake when more substrate is added. The straw's structure, including its rigidity and porosity, also affects how well nutrients and moisture are distributed, which influences microbial access during fermentation.

The data (Table 1) and the 3D plot in Fig. S2 show that increasing the total amount of substrate leads to higher overall LPc production. However, when the results are expressed as production per gram of initial substrate, the highest production were achieved in the triplicate using 12 g of WOC and 6 g of molasses. This suggests that beyond a certain point, additional substrate is not fully utilised under these conditions, likely due to limited accessibility within the solid matrix. Therefore, the tested substrate loading represents a practical optimum for maximising LPc production while ensuring effective substrate use under the current process conditions.

The optimal conditions were experimentally validated in triplicate, resulting in 2.85 ± 0.04 Δlog CFU and 0.94 ± 0.02 g of total LPc (equivalent to 24.9 mg LPc g^{-1} DM). The model prediction was 1.03 g LPc, with a 95 % confidence interval of 0.89–1.17 g, which includes the experimental value, and validates its predictive capacity.

Table 2
ANOVA results for the model when LPc production was used as outcome.

Source	Sum of Squares	df	Mean Square	F-value	p-value
Model	0.4463	3	0.1488	10.86	0.005*
A-WOC	0.1557	1	0.1557	11.37	0.012*
B-MOL	0.0510	1	0.0510	3.73	0.095*
AB	0.1968	1	0.1968	14.37	0.007*
Pure Error	0.0959	7	0.0137		
Cor Total	0.5422	10			

* Significant parameters ($p < 0.05$).

3.2.2. Effect of temperature

The effect of the temperature on biosurfactant and CFU production was also tested in 0.5 L SSF reactors set to isothermal operation at 30, 40, 50 and 60ºC. Figs. 4A and 4B show the sOUR and COC. The maximum sOUR values occurred at approximately 24 and 48 h for 40, 50 and 60ºC. The fermentation at 50°C exhibited the highest sOUR (2.1 ± 0.1 mg O_2 g^{-1} DM h^{-1}), followed by 40°C (1.9 ± 0.2 mg O_2 g^{-1} DM h^{-1}) and 60°C (1.0 ± 0.1 mg O_2 g^{-1} DM h^{-1}), respectively. The corresponding COC values were 99.6, 66.4, and 46.3 mg O_2 g^{-1} DM, respectively, with a minimum oxygen concentration of 18 % in the exhausted airflow.

At 30°C, the fermentation showed a long lag phase (48 h) and very low sOUR values (below 0.6 ± 0.1 mg O_2 g^{-1} DM h^{-1}), indicating that mesophilic temperatures are less favourable for this thermophilic strain, which was originally isolated at 50°C. This low metabolic activity at 30°C is consistent with the known temperature sensitivity of thermophiles. The sOUR profiles at 40°C and 50°C were very similar, with both showing their maximum values within less than one day of difference. The slightly higher sOUR at 50°C likely reflects the optimal temperature for enzymatic activity and metabolism of *B. subtilis* CBI-7S1. Maintaining fermentation temperatures between 40°C and 50°C supports higher microbial activity, as reflected by higher sOUR values under these conditions.

A modified Gompertz model was successfully fitted to the experimental COC data at the different incubation temperatures (Fig. S3). The fits showed excellent agreement with the observations, with coefficients of determination (R^2) exceeding 0.99 in all cases. Nevertheless, the estimated COC_{max} values should be interpreted with caution due to the limited availability of experimental data at longer incubation times, preventing full characterisation of the plateau phase.

The adjusted parameters are presented in Table 3. The lag phase was markedly longer at 30°C (61.8 h) compared to higher temperatures, indicating a slower microbial adaptation under milder thermal conditions. Conversely, the shortest lag was observed at 60°C (17.6 h). The maximum oxygen consumption rate ($Rate_{max}$) increased with temperature up to 50°C, where it reached the highest value (1.87 mg O_2 g^{-1}DM h^{-1}), suggesting an optimal temperature for microbial activity near this level. At 60°C, both the maximum rate and COC declined, possibly reflecting thermal inhibition effects, despite the shorter lag phase.

Fig. 4C shows the LPc production, CFU counts, and pH after 4 days of SSF. The pH remained stable around 6.5–7.0 across all temperatures, consistent with values reported for Bacillus in SSF [28]. Viable cell counts (Δlog CFU) were significantly lower at 30°C, while there were no significant differences between 40, 50, and 60°C, suggesting that the process can be scaled within this temperature range without significant loss of viability. The highest biosurfactant production occurred at 50°C (25 mg LPc g^{-1} DM) with comparable concentration at 40 and 60°C (around 23 mg g^{-1} DM), and the lowest concentration at 30°C. These concentrations fall within the expected range for Bacillus strains in SSF [29–31], supporting the viability of using agro-industrial residues, with production comparable to those obtained using refined substrates but at significantly lower material cost.

3.3. Thermophilic solid-state fermentation at pilot scale

3.3.1. Temperature evolution during the SSF

The temperature was continuously monitored during the SSF using sensors placed throughout the solid matrix. The results are plotted in Fig. 5A. In general, the sensors located at the upper part of the bed (sensors 7, 8, and 9) recorded lower temperatures than those placed in other regions. This may be attributed to the reactor's design, where the presence of an air gap between the surface of the mixture and the uninsulated lid could enhance convective heat loss. However, the middle

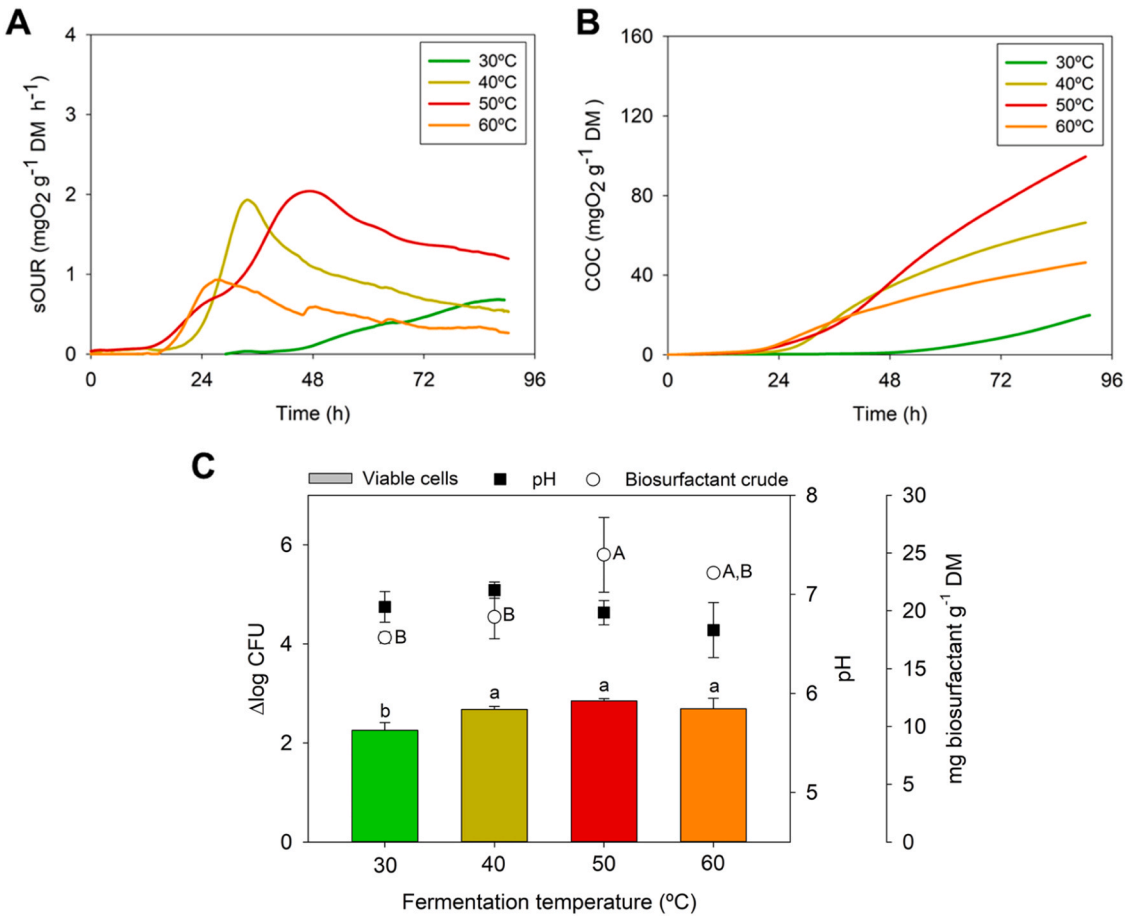

Fig. 4. (A) Specific oxygen uptake rate (sOUR) of CBI-7S1 in SSF and (B) cumulative oxygen consumption (COC) profiles, for the fermentations at the different temperatures tested. (C) Effect of fermentation temperature (30–60°C) on viable cell counts, pH, and biosurfactant production. Means that do not share a common letter are significantly different ($p < 0.05$) for each fermentation temperature, $^{A, B}$ indicate differences in LPc production and $^{a, b}$ indicate differences in CFU.

Table 3
Modified Gompertz model parameters at different fermentation temperatures.

	60ºC	50ºC	40ºC	30ºC
COC_{max} (mg O_2 g^{-1}DM)	48,71	118,65	67,80	63,93
$Rate_{max}$ (mg O_2 g^{-1}DM h^{-1})	0,84	1,87	1,42	0,67
Lag phase (h)	17,59	29,13	24,73	61,80
R^2	0,9970	0,9995	0,9968	0,9992

and lower sections of the reactor maintained relatively stable temperatures between 35°C and 45°C after the first 24 h. These temperature trends align with previously reported profiles in SSF [32,33].

Although the process temperature did not reach thermophilic conditions (45–60°C), for most of the time, it remained around 40°C, which is still within the range where the microorganism could grow effectively at a laboratory scale. In fact, temperatures above 40°C were recorded for 47 % of the fermentation duration in the middle and lower sections of the reactor

Fig. 5B shows the temperature profiles along the height of the reactor at three different fermentation times. At the start of the fermentation, the mixture was approximately 35°C throughout the bed, with a slight increase in temperature observed in the lower section, likely due to the inflow of warm air into the reactor. Subsequently, due to the microorganism's metabolic activity, the temperature across almost the entire solid-packed bed increased over 40°C, reaching its maximum at 48 h, which coincided with the maximum oxygen consumption rate (Fig. 6). Finally, at 96 h, as biological activity declined, heat gradually dissipated, with the mixture evidently cooling, particularly in the top section.

3.3.2. *Fermentation performance*

Figs. 6 and 7 show the evolution of process parameters in *B. subtilis* CBI-7S1 SSF using MOL and WOC wastes as nutrient sources. During the first 10 h, there is no significant change in O_2 consumption, which corresponds to the microorganism's lag phase. Subsequently, oxygen consumption progressively increases, reaching a maximum of 3.1 mg O_2 g^{-1} DM h^{-1} at approximately 48 h. Since oxygen uptake is closely linked to microbial metabolic activity, monitoring sOUR can provide an indirect indication of microbial growth in the reactor.

The maximum values of sOUR and COC were slightly higher at the pilot scale than at the 0.5 L scale. At the end of the laboratory-scale fermentation at 40°C, the moisture content was about 40 %, while at the pilot scale it exceeded 50 %. This higher moisture content at the pilot scale likely increased water activity and enhanced nutrient diffusivity within the substrate, factors that can support higher microbial activity under SSF conditions.

In large-scale reactors, water distribution is often uneven due to evaporation, condensation, and airflow patterns, potentially leading to localised drying or excess moisture in certain zones. In this case, some heterogeneity was observed across the fermented solid (Fig. 7A). The 50 L reactor maintained a stable and even higher moisture content in the upper half of the matrix compared to both the initial and lab-scale moisture levels. This was probably due to lower water evaporation in the upper region of the packed bed and condensation on the reactor lid, causing water droplets to fall back onto the bed surface. This likely enhanced metabolic activity and oxygen consumption. However,

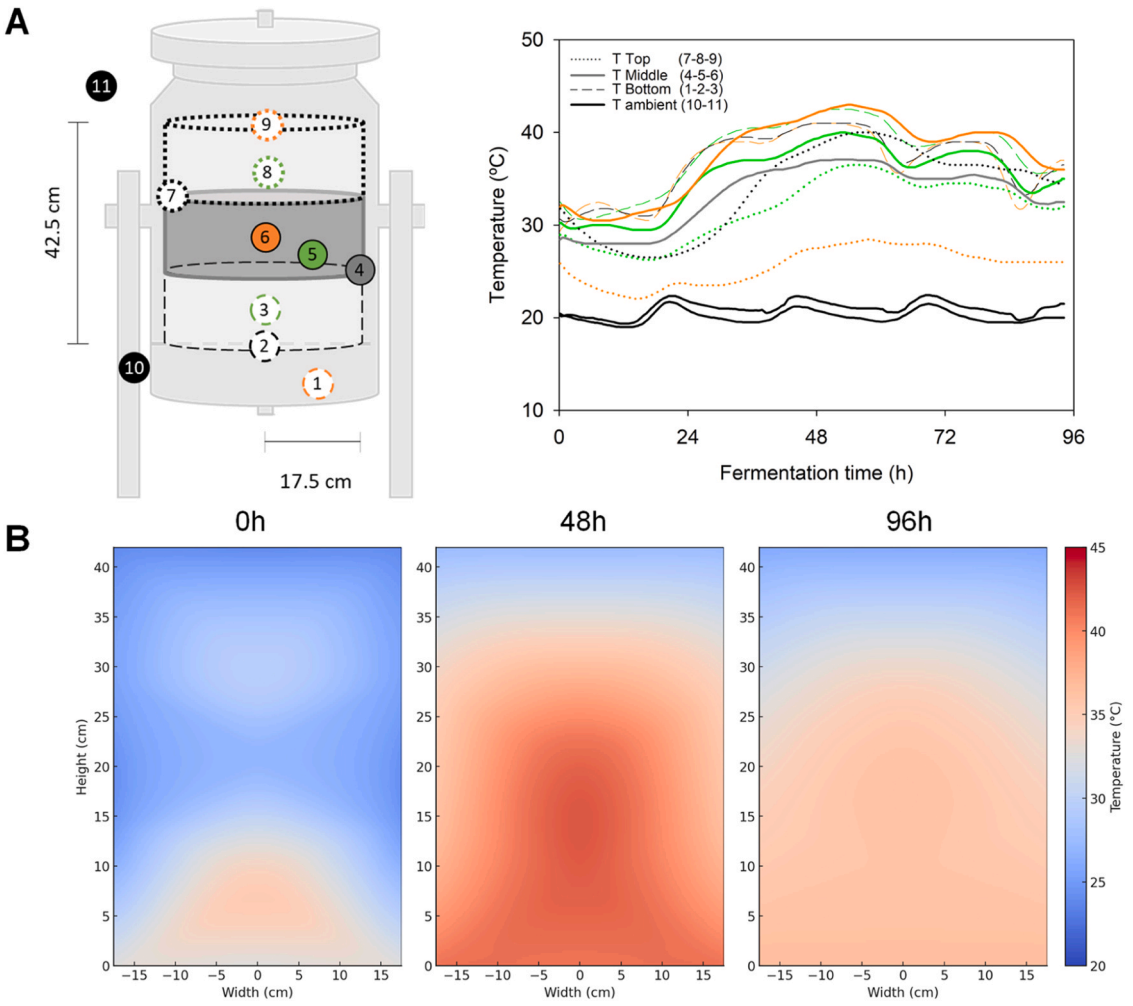

Fig. 5. Temperature profiles of the solid mix in the pilot scale reactor. (A) Temperature evolution during fermentation at different points in the reactor, (B) Heatmap of the solid matrix inside the reactor at different fermentation times.

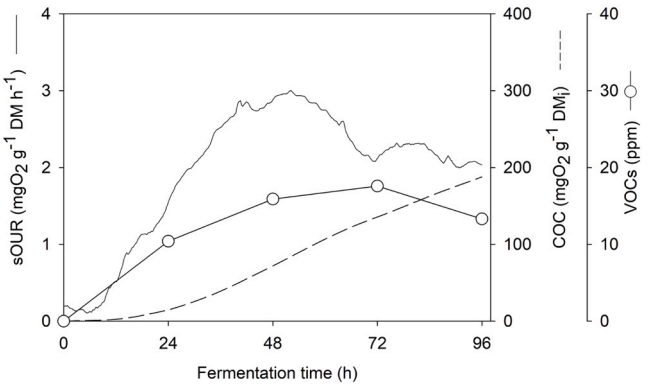

Fig. 6. Analysis of oxygen consumption and VOCs emissions at the outlet of the 50 L reactor during fermentation. Specific oxygen uptake rate (sOUR) and volatile organic compounds (VOCs) concentration are shown.

moisture levels seemed adequate to maintain oxygen diffusion and aerobic conditions in the SSF system, as the substrate near the top was still soft and granular when the bioreactor was opened [6]. Additionally, an increase in moisture was observed along the lateral sections, likely caused by condensed water running down the reactor walls, thereby humidifying the solid.

A reduced airflow rate per kilogram of dry matter was supplied to the larger reactor 20.4 L h^{-1} kg^{-1} DM compared to the lab scale 35.3 L h^{-1} kg^{-1} DM to avoid excessive water evaporation and drying of the solid bed. Despite the lower specific airflow rate, the process remained under aerobic conditions throughout the entire operation period, with oxygen levels in the exhausted air ranging between 19.2 % and 20.9 %. Nevertheless, the results remain consistent with previous studies, reinforcing the idea that maintaining optimal moisture levels and carefully adjusting aeration strategies with humid air are crucial factors in SSF scale-up [16].

In parallel, ammonia, H_2S and total VOCs were analysed to provide insights for further inventories needed to techno-economic analysis and life cycle assessment of the process. No NH_3 or H_2S were detected. VOCs were present, as previously reported in the literature for *Bacillus* strains, such as *Bacillus subtilis* [34,35]. The emission of these VOCs follows a similar trend to oxygen consumption, suggesting a potential correlation with metabolic activity as primary metabolites. The presence of these compounds in the solid matrix – including acids, alcohols, ketones, benzothiazoles, and others [34–36] – could be evaluated to increase the potential of the fermented solid at the end of the fermentation process for the agricultural sector. It has been reported that these compounds exhibit antifungal properties and can act as plant growth stimulants [37–39].

As expected from the oxygen consumption profile, a significant increase in viable *B. subtilis* cells was observed at the end of the fermentation. At the pilot scale, CFU increased by two orders of magnitude (Fig. 7B), which was slightly lower than the 2–3.5 orders observed at the

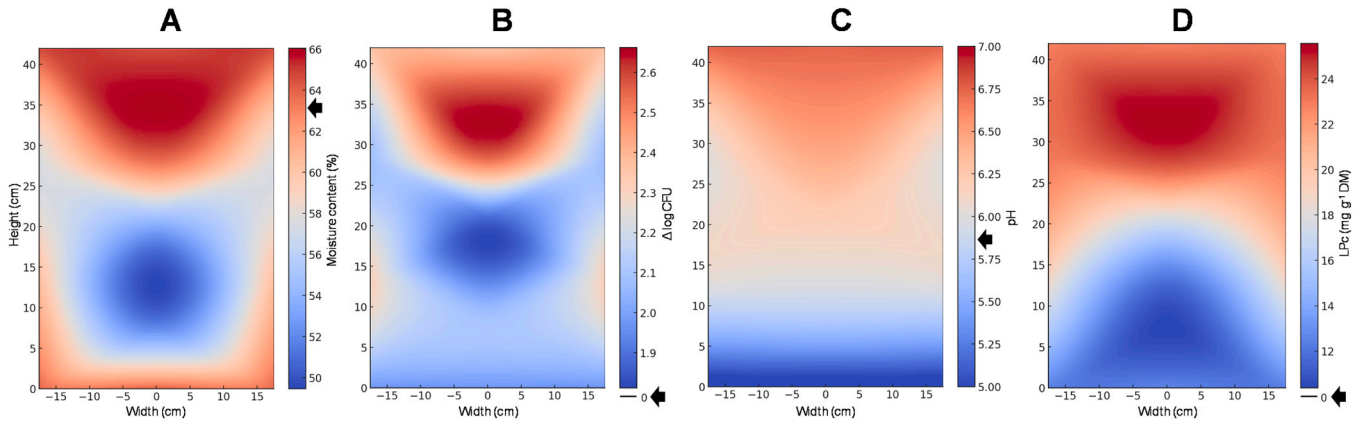

Fig. 7. Spatial distribution of the parameters analysed at the end of fermentation (4 days) in the 50 L reactor. A longitudinal section of the reactor is shown with extrapolated experimental data for (A) moisture content %, (B) Δ log CFU, (C) pH and (D) LPc production. The black arrows indicate the parameter value at the beginning of the fermentation.

lab scale. This difference likely reflects suboptimal conditions in the pilot-scale bioreactor compared to the laboratory-scale bioreactors. Specifically, the pilot-scale system likely exhibited less uniform moisture content, temperature, and oxygen concentrations throughout the reactor volume, leading to localised microenvironments that were further from optimal values for microbial growth. A positive correlation between final CFU and final moisture content was observed, particularly in the reactor upper section, where higher moisture retention favoured microbial growth. In contrast, the lower section, more exposed to airflow, showed reduced CFU counts due to drying. Optimal growth was observed around 40°C, particularly in the middle and upper regions. To improve microbial performance at scale, future efforts should focus on better humidifying the incoming air, ensuring uniform moisture distribution across the reactor bed.

pH values generally shifted from 5.8 to 6.5–7 by the end of fermentation (Fig. 7C), in agreement with laboratory-scale trends and previous SSF studies involving *Bacillus*. However, the lower section became more acidic, likely due to limited microbial activity and late-stage fungal contamination observed during reactor disassembly. Nonetheless, *Bacillus* CFUs remained detectable in that zone. The elevated temperatures registered during fermentation likely inhibited the growth of opportunistic mesophilic microorganisms. This thermophilic environment may offer a competitive advantage for industrial applications by naturally limiting contamination risks and reducing the need for strict sterility measures.

In the upper section, a qualitative correlation emerged between moisture content, CFU levels, pH, and LPc production (Fig. 7). Higher moisture likely promoted *Bacillus* growth, increasing alkalinity and enhancing biosurfactant production. Oxygen availability may have further supported this effect. In contrast, lower LPc concentration in the central-lower region may be attributed to less moisture content and possible compaction observed at the end of the fermentation [33]. In any case, the range of LPc concentration achieved in the reactor was between 15 and 25 mg LPc g^{-1}DM, consistent with the concentration achieved previously at lab scale.

3.4. Biosurfactant characterisation

The relative amounts of the different biosurfactants were calculated according to the area of peaks identified, considering the sum of the areas of all peaks detected. As shown in Table 4, the LPc content a mixture of different congeners of surfactin, iturin and fengycin, all of them previously reported by *Bacillus* strains [38–41]. The possible sequence associated with each mass was estimated according to the literature. The most abundant congeners were C_{14} surfactin [Leu/Ile-Val-Val] (27.3 %) and C_{15} fengycin [Glu-Om-Tyr-Thr-Glu-Ala-Pro-Gln-Tyr-Ile] (27.4 %).

Surface tension properties of LPc were tested under varying concentrations, pH, temperature, and NaCl levels. The relationship between LPc concentration and ST (Fig. 8 A) revealed a characteristic trend where ST decreased as the concentration increased. CMC of 0.16 g L^{-1} was determined, with a corresponding ST of 46.9 mN m^{-1}, This is similar to LPc produced by *Bacillus rugosus* strains, where CMC of 0.1 g L^{-1} has been reported [43]. Above this concentration, surface tension decreased less sharply, indicating micelle formation and interface saturation. Beyond the CMC, the ability of biosurfactants to reduce surface tension typically stabilises, as reported previously [44,45]. Despite reducing the ST of water from 72.26 mN m^{-1} to 46.89 mN m^{-1} at a relatively low concentration, other reports have achieved even lower TS values. This could be attributed to the LPc not being fully purified, potentially containing other proteins or molecules that influence the measurement. However, the product obtained in this process has a higher sustainability potential than other biosurfactants, as it uses only waste materials as substrates and avoids organic solvents during extraction. This significantly reduces the environmental impact typically associated with biosurfactant production. The environmental benefits of this process will be evaluated in future studies.

In the following measurements, ST measurements were performed at an LPc concentration over 15 % above the estimated CMC. In Fig. 8B, the highest ST values were observed at pH 5–6, indicating reduced biosurfactant efficiency. This behaviour is characteristic of lipopeptides

Table 4
Detected congeners of lipopeptide biosurfactants produced at 50 L reactor by SSF using *B. subtilis* CBI-7S1.

Lipopeptide biosurfactants	$[M + H]^+$	Reported *m/z*	Possible sequence	Relative quantity (%)	Ref.
Surfactin	1055.5397	1055.53	C_{15} [Glu–Leu/Ile–Leu–Val–Asp–Leu–Leu/Ile]	8.5	[24]
	1008.6588	1008.66	C_{13} [Leu/Ile-Val-Leu/Ile]	13.0	[40]
	1022.6741	1022.67	C_{14} [Leu/Ile-Val-Val]	27.3	[40]
	1036.6899	1036.72	C_{15} [Glu-Leu/Ile-Leu/Ile-Val-Asp-Leu/Ile-Leu]	17.3	[41]
Iturin	1113.5813	1112.60	C_{19} [Asn–Tyr–Asn–Gln–Pro–Asn–Ser]	6.5	[42]
Fengycin	1468.6420	1468.40	C_{15} [Glu-Om-Tyr-Thr-Glu-Ala-Pro-Gln-Tyr-Ile]	27.4	[24]

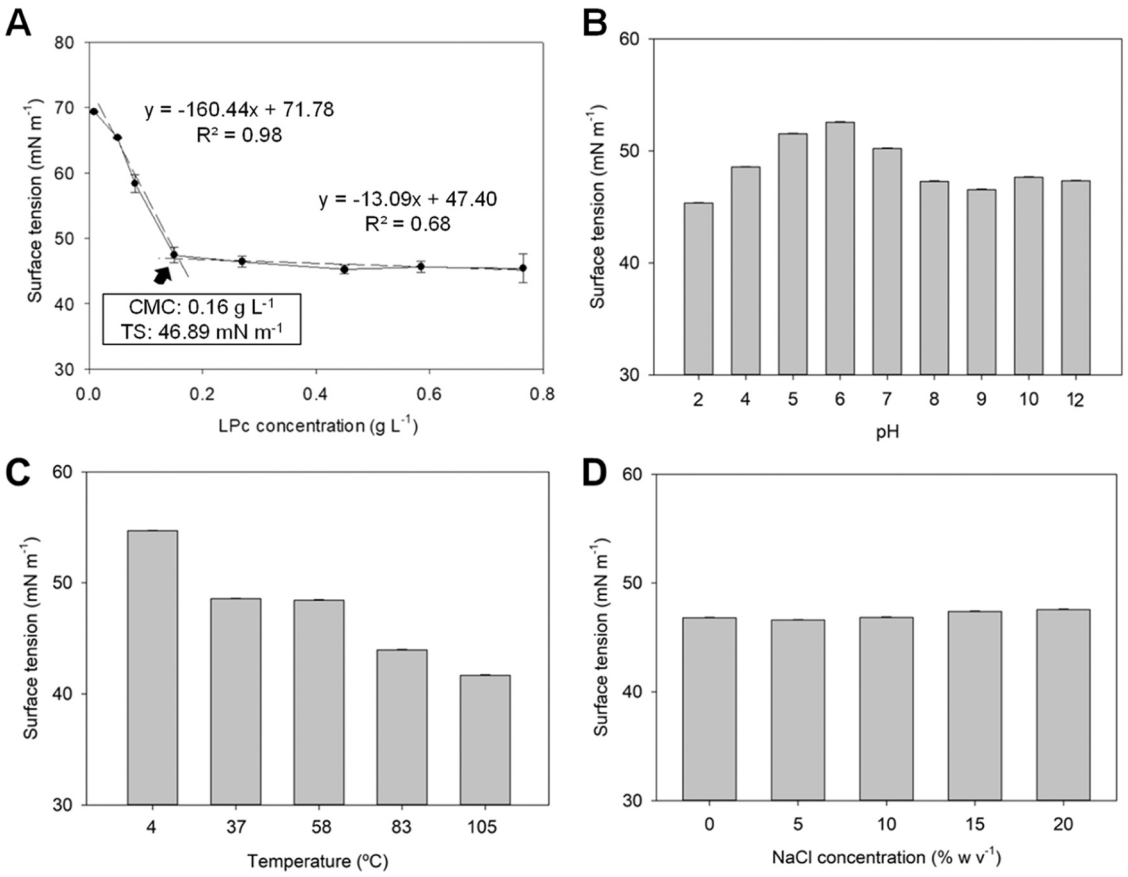

Fig. 8. (A) Surface tension (ST) values for LPc extracted from fermented solid by *B. subtilis* CBI-7S1 from 50 L reactor (black arrow indicates CMC estimation). Influence of pH (B), temperature (C) and salinity (D) to the ST over 15 % above the estimated CMC. All measurements were performed at 23°C, excluding results presented in fig. C.

such as surfactin, which has a net zero charge near pH 5. At this pH, its solubility decreases, and adsorption at the air-water interface is reduced [46]. Minimal electrostatic repulsion at this pH favours micelle aggregation in bulk, thus increasing ST. Under more acidic (pH $<$ 5) or alkaline (pH $>$ 7) conditions, surfactin gains a positive or negative charge, enhancing solubility and interfacial activity, leading to lower ST. Notably, ST remained low even at highly alkaline pH ($\geq$10), possibly due to stabilisation of its amphipathic structure. In any case, ST remained lower than pure water ST at every pH tested.

As temperature increased from 4°C to 105°C (Fig. 8 C), ST progressively decreased, in line with the expected thermal behaviour of aqueous systems. This reduction may be further enhanced by improved molecular mobility and dispersion of the biosurfactant at higher temperatures. [47]. Notably, ST remained low even at 105°C, due to biosurfactant retaining its surface activity under thermal stress, which supports its potential for industrial applications at elevated temperatures [48]. The LPc also showed salt tolerance (Fig. 8D), as ST remained nearly constant across a wide range of NaCl concentrations (5–20 % w/v). The possibility of keeping surface activity under high salinity conditions highlights its potential application in environments such as marine biotechnology [49], enhanced oil recovery [50,51], and bioremediation in saline-contaminated sites [52]. Also, this extract could be a promising candidate in oil production for long-term chemical injection in high-temperature high-salinity reservoirs, where tens of tons of surfactant may be required per well, depending on the reservoir characteristics and operational conditions [48,53].

4. Conclusions

The feasibility of scaling up lipopeptide biosurfactant production using a thermophilic microorganism in SSF packed-bed bioreactors was successfully demonstrated. The process was effectively reproduced at both 0.5 L and 50 L scales using MOL and WOC as substrates, showing a robust and reproducible performance despite temperature gradients. Moisture content was identified as a critical factor influencing fermentation, while oxygen consumption proved a reliable monitoring parameter. The 50 L experiment showed that the thermophilic operating conditions could minimise contamination risks and mitigate heat-related inhibition during fermentation. In addition, surface tension was evaluated under different pH, temperature, and salinity conditions, highlighting its potential for industrial applications. UHPLC–ESI–MS analysis further revealed the presence of surfactin, fengycin, and iturin congeners, demonstrating the diversity of lipopeptides produced.

This study contributes to demonstrating the potential of thermophilic microorganisms for scalable SSF biosurfactant production, providing a practical step towards industrial implementation of sustainable bioprocesses.

CRediT authorship contribution statement

Adriana Artola: Writing – review & editing, Supervision, Conceptualization. **Jose Bueno-Mancebo:** Writing – original draft, Methodology, Investigation, Formal analysis, Data curation, Conceptualization. **Teresa Gea:** Writing – review & editing, Project administration, Funding acquisition, Conceptualization. **Raquel Barrena:** Writing – review & editing, Supervision, Conceptualization. **Syeda Amna Farooq:** Writing – review & editing, Methodology.

Declaration of Competing Interest

The authors declare that they have no known competing financial interests or personal relationships that could have appeared to influence the work reported in this paper.

Acknowledgements

The authors are grateful to the Spanish Ministerio de Ciencia e Innovación (Project SOLSTICE, PID2023–146978OB-100) for the financial support. José Antonio Bueno Mancebo thanks the Spanish Ministerio de Ciencia e Innovación for his pre-doctoral scholarship (FPI PRE2021- 097852).

Appendix A. Supporting information

Supplementary data associated with this article can be found in the online version at doi:10.1016/j.bej.2025.110037.

Data Availability

Data will be made available on request.

References

[1] S.A. Qamar, S. Pacifico, Cleaner production of biosurfactants via bio-waste valorization: A comprehensive review of characteristics, challenges, and opportunities in bio-sector applications, J. Environ. Chem. Eng. 11 (6) (2023), https://doi.org/10.1016/j.jece.2023.111555.
[2] I.M. Banat, Q. Carboue, G. Saucedo-Castaneda, J. de Jesus Cazares-Marinero, Biosurfactants: The green generation of speciality chemicals and potential production using Solid-State fermentation (SSF) technology, Bioresour. Technol. 320 (Pt A) (2021) 124222, https://doi.org/10.1016/j.biortech.2020.124222.
[3] J. Bueno-Mancebo, E. Eras-Muñoz, T. Gea, A. Artola, R. Barrena, Preliminary study on novel sustainable production of mannosylerythritol lipids by solid-state fermentation, Environ. Technol. Innov. 38 (2025), https://doi.org/10.1016/j.eti.2025.104144.
[4] S. Arora, R. Rani, S. Ghosh, Bioreactors in solid state fermentation technology: Design, applications and engineering aspects, J. Biotechnol. 269 (2018) 16–34, https://doi.org/10.1016/j.jbiotec.2018.01.010.
[5] D.A. Mitchell, H.A. Ruiz, N. Krieger, A Critical Evaluation of Recent Studies on Packed-Bed Bioreactors for Solid-State Fermentation, Processes 11 (3) (2023), https://doi.org/10.3390/pr11030872.
[6] David A. Mitchell, Marin Berovič, N. Krieger, Solid-State Fermentation Bioreactors, Springer Berlin Heidelberg, 2006, https://doi.org/10.1007/3-540-31286-2.
[7] M.O. Bamidele, M.B. Bamikale, E. Cárdenas-Hernández, M.A. Bamidele, G. Castillo-Olvera, J. Sandoval-Cortes, C.N. Aguilar, Bioengineering in Solid-State Fermentation for next sustainable food bioprocessing, Sustainability 6 (2025), https://doi.org/10.1016/j.nxsust.2025.100105.
[8] A.G. Corrêa, P. de Oliveira Rodrigues, L.C.B. de Azevedo, D. Pasquini, M.A. Baffi, Reuse of grape pomace and wheat bran for biosynthesis of on-site lignocellulose-degrading enzymes by trametes villosa and trichoderma asperellum under solid state fermentation, Waste Biomass.. Valoriz. 15 (8) (2024) 4747–4760, https://doi.org/10.1007/s12649-024-02502-7.
[9] G. Sinshaw, J. P R, S. J M, A. Ayele, Isolation and characterization of polygalacturonase producing thermophilic Aspergillus niger isolated from decayed tomato fruits, J. Exp. Biol. Agric. Sci. 12 (3) (2024) 379–389, https://doi.org/10.18006/2024.12(3).379.389.
[10] H. Zhang, J. Wu, M. Zhang, Y. Sun, Systematic optimization of cellulases production and extraction by Sporotrichum thermophile mutant strain TH3-9 and application in enzymatic hydrolysis of corn stover, Environ. Technol. Innov. 36 (2024), https://doi.org/10.1016/j.eti.2024.103868.
[11] S. Wang, Z. Wang, N. Wang, S. Wang, S. Zeng, Z. Xu, D. Liu, X. Zhao, F. Liu, J. Xu, Y. Cai, H. Ying, Efficient conversion of corn straw to feed protein through solid-state fermentation using a thermophilic microbial consortium, Waste Manag 194 (2025) 298–308, https://doi.org/10.1016/j.wasman.2025.01.023.
[12] European Commission, Report from the Commission to the European Parliament, the Council, the European and Social Committee and the Committee of the Regions on the implementation of the Circular Economy Action Plan, 2019.
[13] D. Ciurko, Z. Czyznikowska, A. Kancelista, W. Laba, T. Janek, Sustainable Production of biosurfactant from agro-industrial oil wastes by bacillus subtilis and its potential application as antioxidant and ACE Inhibitor, Int J. Mol. Sci. 23 (18) (2022), https://doi.org/10.3390/ijms231810824.
[14] K. Gautam, P. Sharma, V.K. Gaur, P. Gupta, U. Pandey, S. Varjani, A. Pandey, J.W. C. Wong, J.-S. Chang, Oily waste to biosurfactant: a path towards carbon neutrality and environmental sustainability, Environ. Technol. Innov. 30 (2023), https://doi.org/10.1016/j.eti.2023.103095.
[15] J. Bueno-Mancebo, A. Artola, R. Barrena, F. Rivero-Pino, Potential role of sophorolipids in sustainable food systems, Trends Food Sci. Technol. 143 (2024), https://doi.org/10.1016/j.tifs.2023.104265.
[16] S.A. Farooq, R. Barrena, T. Gea, Mining of thermophilic biosurfactant producers for solid-state fermentation, J. Environ. Chem. Eng. 12 (5) (2024), https://doi.org/10.1016/j.jece.2024.114084.
[17] E. Eras-Munoz, T. Gea, X. Font, Carbon and nitrogen optimization in solid-state fermentation for sustainable sophorolipid production using industrial waste, Front Bioeng. Biotechnol. 11 (2023) 1252733, https://doi.org/10.3389/fbioe.2023.1252733.
[18] L. Mejias, A. Cerda, R. Barrena, T. Gea, A. Sánchez, Microbial Strategies for Cellulase and Xylanase Production through Solid-State Fermentation of Digestate from Biowaste, Sustainability 10 (7) (2018), https://doi.org/10.3390/su10072433.
[19] A. Cerda, L. Mejias, T. Gea, A. Sanchez, Cellulase and xylanase production at pilot scale by solid-state fermentation from coffee husk using specialized consortia: The consistency of the process and the microbial communities involved, Bioresour. Technol. 243 (2017) 1059–1068, https://doi.org/10.1016/j.biortech.2017.07.076.
[20] P. Jiménez-Peñalver, T. Gea, A. Sánchez, X. Font, Production of sophorolipids from winterization oil cake by solid-state fermentation: Optimization, monitoring and effect of mixing, Biochem. Eng. J. 115 (2016) 93–100, https://doi.org/10.1016/j.bej.2016.08.006.
[21] P.B. Leege, Introduction of test methods for the examination of composting and compost, in: Beneficial co-utilization of agricultural, municipal and industrial by products, Springer, 1998, pp. 269–282, https://doi.org/10.1007/978-94-011.
[22] D. Maass, I. Moya Ramírez, M. García Román, E. Jurado Alameda, A.A. Ulson de Souza, J.A. Borges Valle, D. Altmajer Vaz, Two-phase olive mill waste (alpeorujo) as carbon source for biosurfactant production, J. Chem. Technol. Biotechnol. 91 (7) (2015) 1990–1997, https://doi.org/10.1002/jctb.4790.
[23] G. Gautam, A Cost Effective Strategy for Production of Bio-surfactant from Locally Isolated Penicillium chrysogenum SNP5 and Its Applications, J. Bioprocess. Biotech. 04 (06) (2014), https://doi.org/10.4172/2155-9821.1000177.
[24] I. Mnif, R. Segovia, A. Bouallegue, D. Ghribi, F. Rabanal, Identification of different lipopeptides isoforms produced by bacillus mojavensis BI2 and evaluation of their surface activities for potential environmental application, J. Polym. Environ. 31 (6) (2023) 2668–2685, https://doi.org/10.1007/s10924-022-02752-3.
[25] M. Emkani, B. Oliete, R. Saurel, Effect of lactic acid fermentation on legume protein properties, a review, Fermentation 8 (6) (2022), https://doi.org/10.3390/fermentation8060244.
[26] C. Li, Z. Liu, Z. Gong, Z. Bao, J. Zhao, Z.-M. Zhao, Steam explosion enhancing Bacillus subtilis fermentation on lignocellulosic biomass to prepare high-titer microecological agents, Ind. Crops Prod. 226 (2025), https://doi.org/10.1016/j.indcrop.2025.120707.
[27] X. Guan, H. Yao, Optimization of Viscozyme L-assisted extraction of oat bran protein using response surface methodology, Food Chem. 106 (1) (2008) 345–351, https://doi.org/10.1016/j.foodchem.2007.05.041.
[28] W. Li, T. Wang, Effect of solid-state fermentation with Bacillus subtilis lwo on the proteolysis and the antioxidative properties of chickpeas, Int J. Food Microbiol 338 (2021) 108988, https://doi.org/10.1016/j.ijfoodmicro.2020.108988.
[29] M. Bouassida, I. Mnif, I. Hammami, M.A. Triki, D. Ghribi, Bacillus subtilis SPB1 lipopeptide biosurfactant: antibacterial efficiency against the phytopathogenic bacteria Agrobacterium tumefaciens and compared production in submerged and solid state fermentation systems, Food Sci. Biotechnol. 32 (11) (2023) 1595–1609, https://doi.org/10.1007/s10068-023-01274-5.
[30] M. Li, H. Mou, Q. Kong, T. Zhang, X. Fu, Bacteriostatic effect of lipopeptides from Bacillus subtilis N-2 on Pseudomonas putida using soybean meal by solid-state fermentation, Mar. Life Sci. Technol. 2 (2) (2020) 172–180, https://doi.org/10.1007/s42995-020-00028-0.
[31] Z. Zhu, L. Sun, X. Huang, W. Ran, Q. Shen, Comparison of the kinetics of lipopeptide production by Bacillus amyloliquefaciens XZ-173 in solid-state fermentation under isothermal and non-isothermal conditions, World J. Microbiol Biotechnol. 30 (5) (2014) 1615–1623, https://doi.org/10.1007/s11274-013-1587-7.
[32] L. Mejias, D. Ruiz, E. Molina-Peñate, R. Barrena, T. Gea, Bacillus thuringiensis derived biopesticides from biowaste digestate at 290-L demonstration scale through solid-state fermentation, Environ. Technol. Innov. 37 (2025), https://doi.org/10.1016/j.eti.2024.103974.
[33] A. Karimi, S.A. Shojaosadati, P. Hejazi, E. Vasheghani-Farahani, M. Hashemi, Porosity changes during packed bed solid-state fermentation, J. Ind. Eng. Chem. 20 (6) (2014) 4022–4027, https://doi.org/10.1016/j.jiec.2014.01.001.
[34] J. Hu, Z. Su, B. Dong, D. Wang, X. Liu, H. Meng, Q. Guo, H. Zhou, Characterization of a Bacillus subtilis S-16 Thiazole-Synthesis-Related Gene thiS Knockout and Antimicrobial Activity Analysis, Curr. Issues Mol. Biol. 45 (6) (2023) 4600–4611, https://doi.org/10.3390/cimb45060292.
[35] E.G. Poulaki, S.E. Tjamos, Bacillus species: factories of plant protective volatile organic compounds, J. Appl. Microbiol 134 (3) (2023), https://doi.org/10.1093/jambio/lxad037.
[36] J. Grahovac, I. Pajcin, V. Vlajkov, Bacillus VOCs in the context of biological control, Antibiotics 12 (3) (2023), https://doi.org/10.3390/antibiotics12030581.
[37] H.A. Tahir, Q. Gu, H. Wu, W. Raza, A. Hanif, L. Wu, M.V. Colman, X. Gao, Plant growth promotion by volatile organic compounds produced by Bacillus subtilis SYST2, Front Microbiol 8 (2017) 171, https://doi.org/10.3389/fmicb.2017.00171.
[38] K. Wang, Z. Qin, S. Wu, P. Zhao, C. Zhen, H. Gao, Antifungal mechanism of volatile organic compounds produced by bacillus subtilis CF-3 on colletotrichum gloeosporioides assessed using omics technology, J. Agric. Food Chem. 69 (17) (2021) 5267–5278, https://doi.org/10.1021/acs.jafc.1c00640.

[39] Z.A. Awan, A. Shoaib, P.M. Schenk, A. Ahmad, S. Alansi, B.A. Paray, Antifungal potential of volatiles produced by Bacillus subtilis BS-01 against Alternaria solani in Solanum lycopersicum, Front Plant Sci. 13 (2022) 1089562, https://doi.org/10.3389/fpls.2022.1089562.
[40] F. Hu, W. Cai, J. Lin, W. Wang, S. Li, Genetic engineering of the precursor supply pathway for the overproduction of the nC(14)-surfactin isoform with promising MEOR applications, Micro Cell Fact. 20 (1) (2021) 96, https://doi.org/10.1186/s12934-021-01585-4.
[41] S.S. Barale, S.G. Ghane, K.D. Sonawane, Purification and characterization of antibacterial surfactin isoforms produced by Bacillus velezensis SK, AMB Express 12 (1) (2022) 7, https://doi.org/10.1186/s13568-022-01348-3.
[42] J. Vater, B. Kablitz, C. Wilde, P. Franke, N. Mehta, S.S. Cameotra, Matrix-assisted laser desorption ionization–time of flight mass spectrometry of lipopeptide biosurfactants in whole cells and culture filtrates of Bacillus subtilis C-1 isolated from petroleum sludge, Appl. Environ. Microbiol 68 (12) (2002) 6210–6219, https://doi.org/10.1128/AEM.68.12.6210-6219.2002.
[43] G.J. Jeong, D.K. Kim, D.J. Park, K.J. Cho, M.U. Kim, D.K. Oh, N. Tabassum, W. K. Jung, F. Khan, Y.M. Kim, Control of Staphylococcus aureus infection by biosurfactant derived from Bacillus rugosus HH2: Strain isolation, structural characterization, and mechanistic insights, J. Hazard Mater. 480 (2024) 136402, https://doi.org/10.1016/j.jhazmat.2024.136402.
[44] C.R. Guimaraes, I.P. Pasqualino, J.S. de Sousa, F.C.S. Nogueira, L. Seldin, L.V.A. de Castilho, D.M.G. Freire, Bacillus velezensis H2O-1 surfactin efficiently maintains its interfacial properties in extreme conditions found in post-salt and pre-salt oil reservoirs, Colloids Surf. B Biointerfaces 208 (2021) 112072, https://doi.org/10.1016/j.colsurfb.2021.112072.
[45] A. Sani, W.Q. Qin, J.Y. Li, Y.F. Liu, L. Zhou, S.Z. Yang, B.Z. Mu, Structural diversity and applications of lipopeptide biosurfactants as biocontrol agents against phytopathogens: A review, Microbiol Res 278 (2024) 127518, https://doi.org/10.1016/j.micres.2023.127518.
[46] P.-H. Chang, S.-Y. Li, T.-Y. Juang, Y.-C. Liu, Mg-Fe Layered Double Hydroxides Enhance Surfactin Production in Bacterial Cells, Crystals 9 (7) (2019), https://doi.org/10.3390/cryst9070355.
[47] M. Bouassida, I. Ghazala, S. Ellouze-Chaabouni, D. Ghribi, Improved biosurfactant production by bacillus subtilis SPB1 mutant obtained by random mutagenesis and its application in enhanced oil recovery in a sand system, J. Microbiol Biotechnol. 28 (1) (2018) 95–104, https://doi.org/10.4014/jmb.1701.01033.
[48] K. Panthi, K.K. Mohanty, Development of surfactant formulation for high-temperature off-shore carbonate reservoirs, Front Chem. 12 (2024) 1408115, https://doi.org/10.3389/fchem.2024.1408115.
[49] S. Kubicki, A. Bollinger, N. Katzke, K.E. Jaeger, A. Loeschcke, S. Thies, Marine Biosurfactants: Biosynthesis, Structural Diversity and Biotechnological Applications, Mar. Drugs 17 (7) (2019), https://doi.org/10.3390/md17070408.
[50] A. Chafale, A. Kapley, Biosurfactants as microbial bioactive compounds in microbial enhanced oil recovery, J. Biotechnol. 352 (2022) 1–15, https://doi.org/10.1016/j.jbiotec.2022.05.003.
[51] I.A. Purwasena, M. Amaniyah, D.I. Astuti, Y. Firmansyah, Y. Sugai, Production, characterization, and application of Pseudoxanthomonas taiwanensis biosurfactant: a green chemical for microbial enhanced oil recovery (MEOR), Sci. Rep. 14 (1) (2024) 10270, https://doi.org/10.1038/s41598-024-61096-1.
[52] S. Kalvandi, H. Garousin, A.A. Pourbabaee, M. Farahbakhsh, The release of petroleum hydrocarbons from a saline-sodic soil by the new biosurfactant-producing strain of Bacillus sp, Sci. Rep. 12 (1) (2022) 19770, https://doi.org/10.1038/s41598-022-24321-3.
[53] J. Hou, T. Huang, M. Alotaibi, A. AlSofi, Long-term thermal stability of ionic surfactants for improving oil production at high-salinity high-temperature conditions, ACS Omega 9 (10) (2024) 11976–11986, https://doi.org/10.1021/acsomega.3c09734.